Applied Catalysis B: Environmental 317 (2022) 121791

Contents lists available at ScienceDirect

Applied Catalysis B: Environmental

journal homepage: www.elsevier.com/locate/apcatb

Synergistic combination of triazine and phenanthroline moieties in a covalent triazine framework tailored for heterogeneous photocatalytic metal-free C-Br and C-Cl activation

Alberto López-Magano [a], Noelia Salaverri [b], Leyre Marzo [b,c,*], Rubén Mas-Ballesté [a,c,*], Jose Alemán [b,c,*]

[a] Inorganic Chemistry Department, Módulo 7, Universidad Autónoma de Madrid, 28049 Madrid, Spain
[b] Organic Chemistry Department, Módulo 1, Universidad Autónoma de Madrid, 28049 Madrid, Spain
[c] Institute for Advanced Research in Chemical Sciences (IAdChem), Universidad Autónoma de Madrid, 28049 Madrid, Spain

ARTICLE INFO

Keywords:
Covalent triazine framework
CTF
Photochemistry
Photoredox
Dehalogenation

ABSTRACT

We present the design and synthesis of a new covalent triazine framework with high content of N atoms bearing triazine and phenanthroline moieties. This material displays interesting luminescence phenomena and enhanced photoredox activity as a consequence of synergistic combination of both *N*-containing aromatic fragments. As catalytic application, the reduction of a variety of brominated and challenging chlorinated aromatic structures, including persistent organic pollutants such as polybrominated diphenyl ethers, has been performed under light irradiation and room temperature conditions. These chemical transformations follow a photoredox mechanism involving the formation of aryl radicals, that were trapped with different radical acceptors in order to afford the formation of new C-C, C-B and C-P bonds.

1. Introduction

The research on new photoredox systems able to activate different type of bonds in order to afford the synthesis of novel molecules is a main target in modern chemistry [1]. However, it requires reaching adequate oxidation or reduction potentials at the photocatalyst's excited state, that should allow transference of electrons between the organic substrates and the photocatalyst [2]. This feature has been achieved with a variety of catalytic molecules consisting of transition metal compounds such as Ir coordination complexes [3] or organic molecules with extended aromatic structures such as phenyl-phenothiazine [4], rhodamine 6G [5–7] or perylene-diimide derivatives [8], among others [9].

However, such behavior is scarcely found in heterogeneous systems, especially when approaching to the visible-light range [10,11]. Therefore, the quest of organic photocatalytic materials able to activate different chemical bonds with highly demanding redox potentials is a very attractive research playground. The main goal of such materials should be affording new synthetic pathways that would otherwise be prohibitive in the absence of light.

Among the photoredox processes, the activation of carbon-bromine [12], and more specifically, carbon-chlorine bonds [13], with very high reduction potentials represents a challenge mainly achievable by very powerful molecular photoredox catalysts [14,15]. This kind of photocatalytic processes is especially interesting: on the one hand, the synthesis of molecules through the formation of new chemical bonds could be afforded by capture of the generated transient aryl radical [16]; on the other hand, carbon-bromine bonds are found in a wide variety of persistent organic pollutants, being their activation the first step to nullify their harmful effect on the environment [17]. Thus, the obtention of new organic photocatalytic materials able to perform this type of processes seems to be a necessary and coveted target. To this respect, examples consisting on different porous organic materials able to trigger photoreductive dehalogenation reactions are scarcely found in the literature [18]. Among them, different covalent organic frameworks [19–22] and conjugated microporous polymers [23–25] have been able, up to now, to activate phenacyl halides or bromomalonates (see Table S4 of Supporting Information). These substrates have more easily achievable reduction potentials than aryl halides, which are much more challenging to reduce.

* Corresponding authors at: Institute for Advanced Research in Chemical Sciences (IAdChem), Universidad Autónoma de Madrid, 28049 Madrid, Spain.
E-mail addresses: leyre.marzo@uam.es (L. Marzo), ruben.mas@uam.es (R. Mas-Ballesté), jose.aleman@uam.es (J. Alemán).

https://doi.org/10.1016/j.apcatb.2022.121791
Received 9 June 2022; Received in revised form 22 July 2022; Accepted 24 July 2022
Available online 26 July 2022

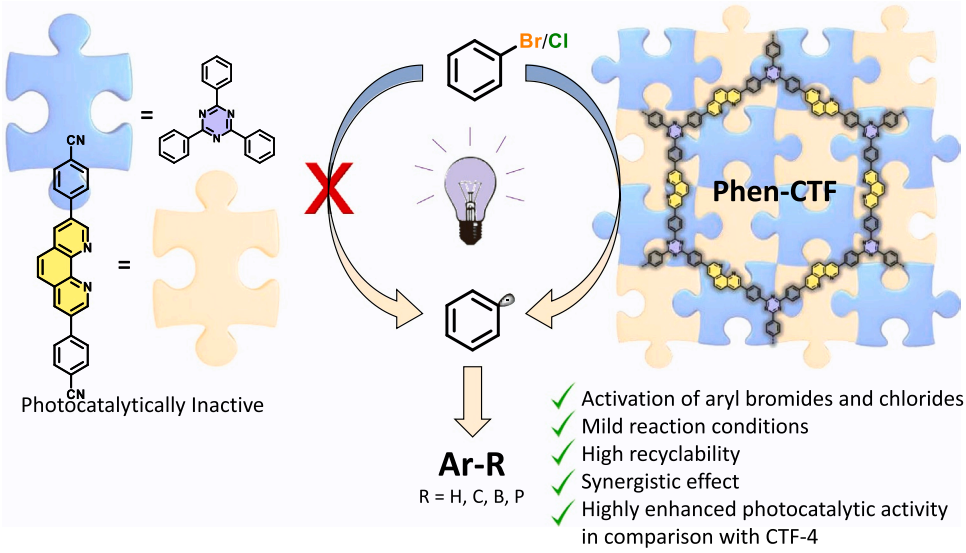

Fig. 1. General idea of this work: synergistic combination of triazine and phenanthroline units to achieve photocleavage of carbon-halogen bonds.

As a promising family of materials with interesting photophysical characteristics, covalent triazine frameworks represent a valuable alternative [26]. These materials are composed by solely organic structures that are assembled through the formation of the 6-membered 1,3,5-triazine ring, that display interesting photocatalytic properties for different applications [27–30]. In organic synthesis field, several CTFs have been used for different light-mediated chemical transformations, such as sulfide [31–35] and benzyl alcohol [36,37] aerobic photooxidations, oxidative coupling of amines [38,39], and C-N couplings in presence of Ni(II) [40], among others [41,42]. The vast majority of these examples consist of oxidation reactions with easily achievable redox potentials (see Table S4 of Supporting Information). However, the precise control of the redox potentials that can be reached by the CTFs' excited states through the design of their structure has yet to be more explored, in order to expand the range of photocatalytic transformations that these materials are capable of carrying out. To this respect, in recent works, it has been suggested that the presence of N atoms in CTFs [43] and related conjugated materials such as COFs [44] has a fundamental role in their photophysical properties and photocatalytic activities. Thus, in this work, we have addressed the increase in conjugation and nitrogen content of a model CTF material such as **CTF-4** [45]. For this purpose, we have predesigned a building block containing phenanthroline scaffolds, which contains additional nitrogen atoms and displays enhanced rigidity. Thus, the use of phenanthroline [46] not only adds N atoms to the CTF structure, but also increases the electronic delocalization in comparison with other materials composed of bipyridines or biphenyls, which have free rotation [47]. Combination of triazine and phenanthroline moieties resulted in a synergistic effect, which accounts for an enhanced activity that cannot be observed with the molecular fragments separately. Therefore, we show that the interplay of triazine and phenanthroline fragments in a new CTF (**Phen-CTF**) allows to activate a variety of C-X (X ═Br, Cl) bonds under visible-light irradiation. As a result, the generation of more complex molecules through the capture of the generated aryl radical by various trapping scaffolds has been performed, affording new C-H, C-C, C-P and C-B bonds. Finally, three emergent persistent organic pollutants containing C-Br bonds were also dehalogenated under soft conditions. Fig. 1.

2. Experimental

2.1. Synthesis of 4,4′-(1,10-phenanthroline-3,8-diyl)dibenzonitrile (1)

3,8-dibromo-1,10-phenanthroline (400 mg, 1.18 mmol), 4-cyanophenylboronic acid (520 mg, 3.54 mmol), potassium carbonate (980 mg, 7.10 mmol) and $Pd(PPh_3)_4$ (272 mg, 0.24 mmol) were introduced into a Schlenk flask equipped with a magnetic stirrer. The flask was subjected to three vacuum-Ar cycles. Then, 10 mL of 1,4-dioxane and 2 mL of distilled water previously degassed were added. The system was heated at 100 ° C during 72 h. Then, the solvent was evaporated under reduced pressure. The solid was triturated with distilled water and filtrated, then dissolved in 250 mL of hot $CHCl_3$. The solution was rapidly filtrated over a plug of celite, rinsed with $CHCl_3$ and evaporated under reduced pressure. Finally, it was washed with cold acetone and dried under vacuum, affording **1** as a pale-yellow solid in 72% yield. ^{1}H NMR (300 MHz, $CDCl_3$) δ 9.45 (d, J = 2.3 Hz, 2 H), 8.47 (d, J = 2.3 Hz, 2 H), 7.97 (s, 2 H), 7.92 (d, J = 8.7 Hz, 4 H), 7.87 (d, J = 8.5 Hz, 4 H). ^{13}C NMR (75 MHz, $CDCl_3$) δ 149.2, 145.7, 145.2, 141.9, 134.2, 134.1, 133.1, 128.7, 128.2, 127.5, 118.5, 112.4, 112.1. Elemental analysis: calculated for $C_{26}H_{14}N_4$: C, 81.66; H, 3.69; N, 14.65. Found: C, 81.73; H, 3.75; N, 14.57.

2.2. Synthesis of Phen-CTF

in a 100 mL pear-shaped flask fitted with a Teflon screw cap, 400 mg of 1 were dispersed in 10 mL of dichloromethane under and ultrasound bath for 10 min. Then, 4 mL of trifluoromethanesulfonic acid were added dropwise under an ice bath. The flask was sealed, and the mixture was heated at 100 ° C during 24 h. After cooling down to room temperature, 20 mL of a mixture of EtOH-water 1:1 were added dropwise with gentle stirring. The yellow solid was isolated by centrifugation and repeatedly washed with EtOH-water 1:1 until neutral pH was reached. Then, the material was finally washed with acetone and diethyl ether and dried under vacuum for 24 h. 487 mg obtained (81% yield). For the characterization, see Supporting Information.

2.3. General procedure for the photocatalytic dehalogenation

A vial equipped with a magnetic stir bar was charged with aryl halide **2** (0.1 mmol, 1.0 equiv.), **Phen-CTF** (1.0 mg) followed by MeCN (1.0 mL), NBu_3 (0.5 mmol, 5.0 equiv., 119 μL) and HCOOH (0.5 mmol, 5.0 equiv., 19 μL). The vial was sealed, and degasification was performed via freeze-pump-thaw cycling (3 ×10 min under vacuum). Then, the reaction mixture was irradiated and stirred in the photoreactor equipped with 15 W LEDs of 385 nm that is internally cooled by circulating a cooling liquid at 20 ° C (see S.I. for the photoreactor), which ensures reproducibility and exhaustive control of the reaction conditions

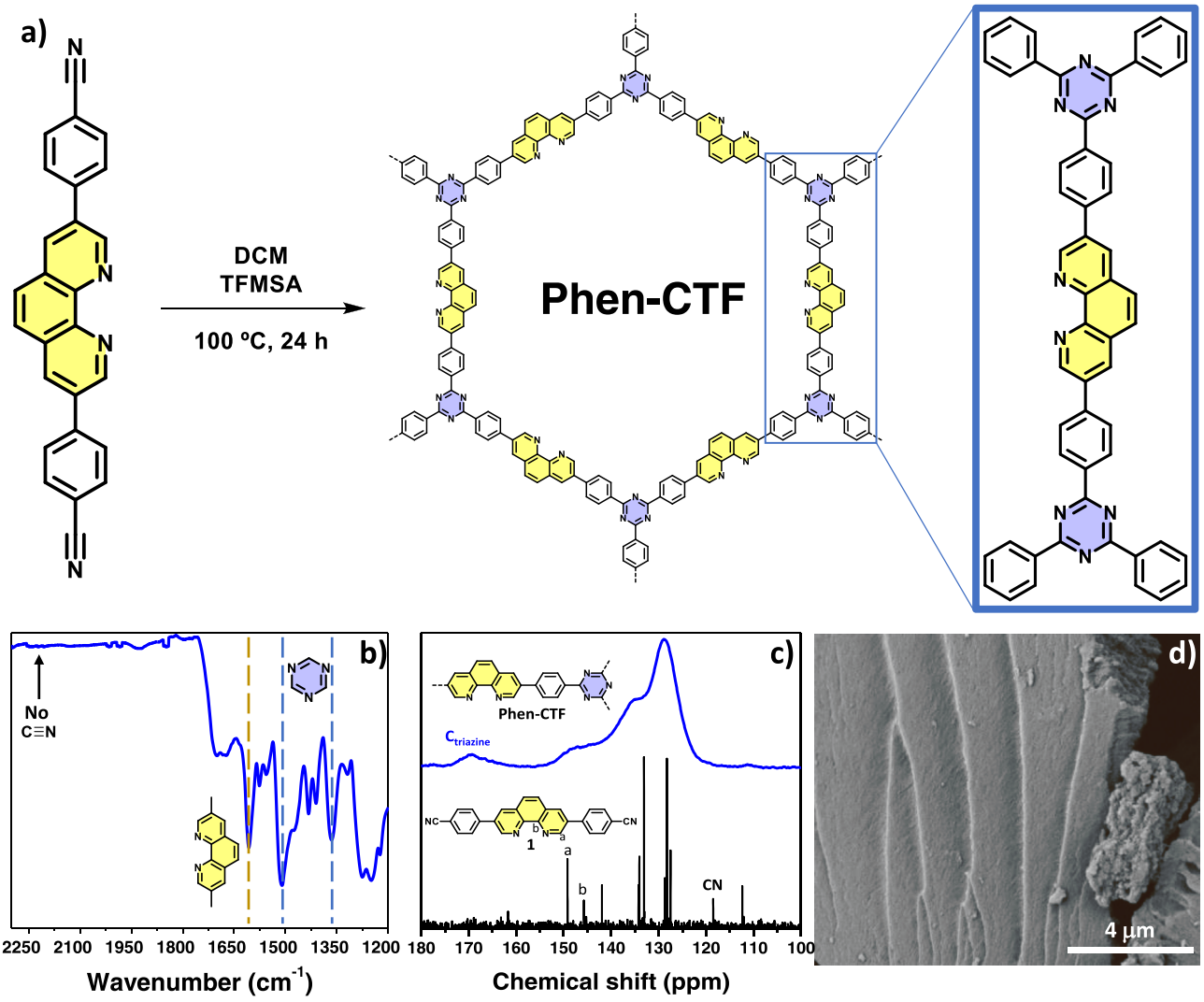

Fig. 2. Synthesis and characterization of **Phen-CTF**. a) Reaction conditions for the synthesis of **Phen-CTF**; b) FTIR spectrum; c) Comparison between ^{13}C NMR of **1** and **Phen-CTF** (for the full range of the spectra, see Figs. S2 and S5 of S.I.); d) SEM image.

for 17 h (aryl bromides) or 72 h (aryl chlorides). After this time, the internal standard was added (1,3,5-trimethoxybenzene) and a 0.1 mL aliquot of the reaction mixture was withdrawn and analyzed by ^1H NMR spectroscopy to calculate the corresponding yields.

2.4. General procedure for the photocatalytic dehalogenation and aryl radical trapping

A vial equipped with a magnetic stir bar was charged with aryl halide **2** (0.1 mmol, 1.0 equiv.), **Phen-CTF** (1.0 mg) followed by DMSO (1.0 mL), NBu_3 (0.2 mmol, 2.0 equiv.) and the radical trapping reagent (pyrrole, *N*-methylpyrrole, *N*-phenylpyrrole, 2,4-dimethylpyrrole, 1,3,5-trimethoxybenzene, triethyl phosphite, bis(pinacolato)diboron, 2.5 mmol, 25.0 equiv.). The vial was sealed, and degasification was performed via freeze-pump-thaw cycling (3 ×10 min under vacuum). Then, the reaction mixture was irradiated and stirred in the photoreactor equipped with 15 W LEDs of 385 nm that is internally cooled by circulating a cooling liquid at 20 ° C, which ensures reproducibility and exhaustive control of the reaction conditions for 17 h (aryl bromides) or 72 h (aryl chlorides). The reaction mixture was concentrated under reduced pressure and purified by column chromatography or the yield was calculated by internal standard (specified in each case).

3. Result and discussion

3.1. Synthesis and characterization of the material Phen-CTF

We firstly performed the synthesis of building block 4,4′-(1,10-phenanthroline-3,8-diyl)dibenzonitrile (**1**) by cross-coupling of 3,8-dibromophenanthroline with 4-cyanophenylboronic acid in presence of potassium carbonate as a base and $Pd(PPh_3)_4$ as catalyst at 100 ° C during 48 h. Then, we proceeded to the synthesis of **Phen-CTF**. To this respect, in the available literature, various methodologies have been developed for CTFs' synthesis, usually involving the use of ionothermal conditions and high temperatures [48]. These conditions allow the isolation of polymers with enhanced crystallinity and porosity from the corresponding nitriles. However, in most of the cases, their photophysical properties are sacrificed, since undesired carbonization processes lead to the formation of black-colored polymers [49]. Thus, we decided to perform the cyclotrimerization of **1** following a double-phase thermal process involving the use of trifluoromethanesulfonic acid (TFMSA) and dichloromethane at 100 ° C. As previously reported, CTF material was obtained through this procedure with excellent photophysical properties [50], but limited porosity and crystallinity (see below).

Initial characterization of **Phen-CTF** was carried out by means of Fourier transformed infrared spectroscopy (FTIR). The formation of the

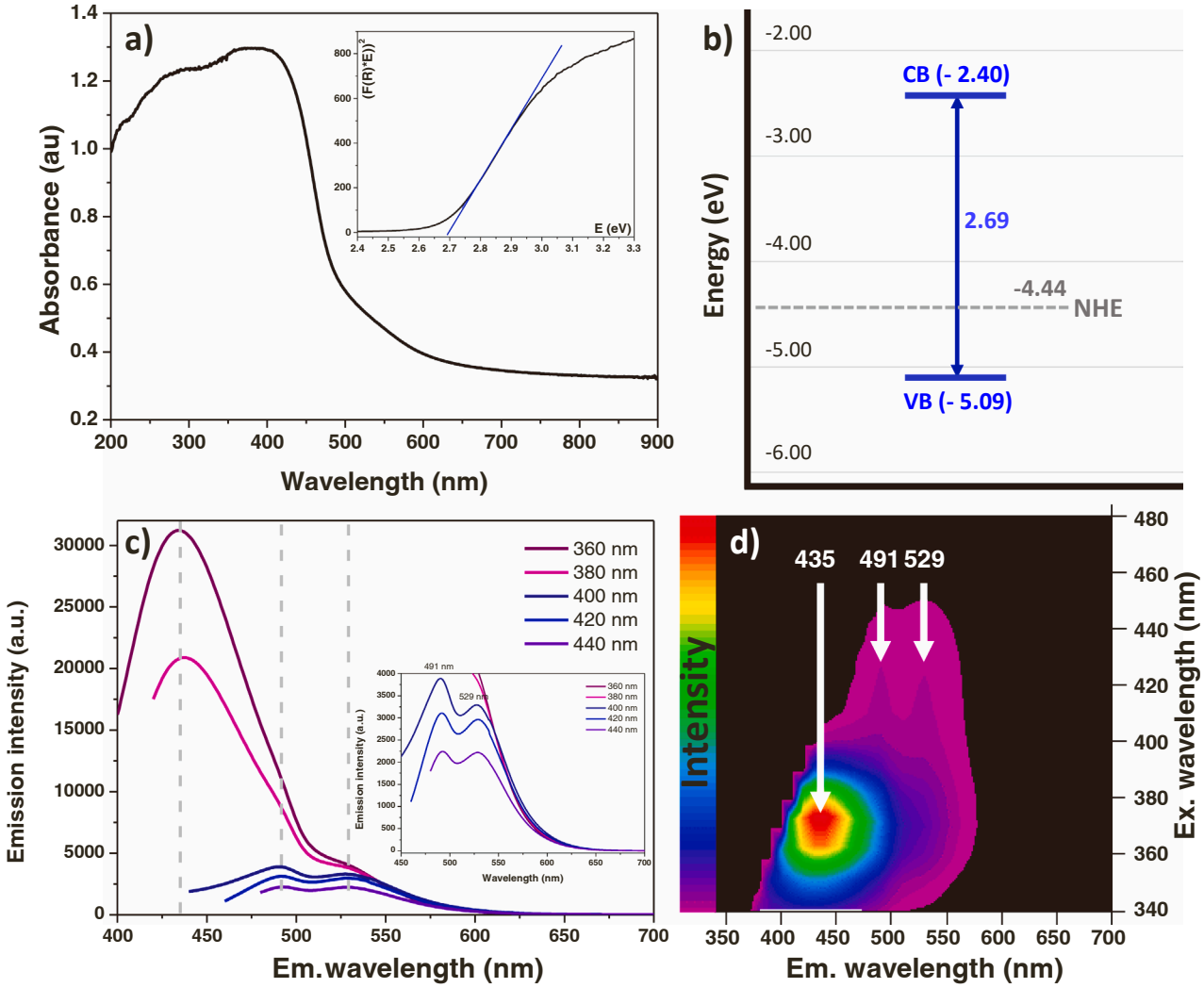

Fig. 3. Study of photophysical properties of **Phen-CTF**. a) DRS spectrum and Kubelka-Munk plot; b) Energy levels; c) Excitation-emission profile; d) Topological map of emissions of **Phen-CTF**.

expected triazinyl material was confirmed by two observations (Fig. 2a): first, the disappearance of the vibration associated to nitrile stretchings at 2229 cm^{-1}; and secondly, the presence of two strong vibrations bands at 1510 and 1361 cm^{-1}, assigned to aromatic C-N stretching and breathing modes of triazine units [39]. Formation of triazine rings was also corroborated by solid-state ^{13}C NMR, obtained by cross polarization magical angle spinning (CP-MAS), where a characteristic peak centered at 170 ppm is assigned to the aromatic carbons of C_3N_3 moiety (Fig. 2b) [51]. The rest of the bands correspond to aromatic carbons present in the framework, as it can be observed from the comparison between the spectra of **Phen-CTF** and **1** [11,46]. Combination of elemental analysis and thermogravimetric analysis (TGA) of **Phen-CTF** allowed to verify the purity of the material and absence of any residual amounts of solvent or TFMSA, matching with the expected formula $C_{39}H_{21}N_6$. TGA also revealed an excellent stability up to 350 ° C under air atmosphere (Fig. S6 of Supporting Information). Regarding crystallinity, powder X-ray diffraction of **Phen-CTF** did not show any diffraction peaks, confirming the amorphous nature of the triazine polymer (Fig. S3). Moreover, its specific Brunauer-Emmett-Teller (BET) surface area, evaluated with N_2 adsorption obtained at 77 K, reached 358 m^2/g, that is in the state-of-the-art of CTFs obtained with this methodology (Fig. S4) [27,39]. Layered microstructure as a result of stacking of 2D architectures is well observed by scanning electron microscopy (SEM).

With regard to the band distribution and energy levels, we conducted diffuse reflectance spectroscopy (DRS) measurements, that revealed a continuous absorption in the UV–visible range up to 440 nm (Fig. 3a). Accordingly, Kubelka-Munk transformed spectra allowed us to estimate the corresponding band gap of **Phen-CTF**, located at 2.69 eV (Fig. S7). Moreover, electrochemical data obtained from the first oxidation signal of cyclic voltammetry curve (Fig. S8) enabled the determination of the valence band (VB) of the material [52,53], which has a value of − 5.09 eV. The combination between the values of VB and band gap determined the energy level of the conduction band, located at − 2.40 eV (Fig. 3b). The high dispersibility of **Phen-CTF** in EtOH allowed us to evaluate its photoluminescence in suspension. Interestingly, a strong emission band was detected at 435 nm (Fig. 3c and d) when excited in the range of 360–380 nm. This phenomenon is directly related to the strong luminescent emission that we observe in the material with the naked eye when irradiated with a conventional near-UV lamp in solid-state (see Fig. S9 of Supporting Information). In addition, as we move to longer excitation wavelengths, two other emission bands centered on 491 and 529 nm were detected. These observations suggest that excited states of different energy can be reached by irradiating in the range of UV–visible light.

3.2. *Photocatalytic application: Aryl radical generation*

The observation of emissions at different energies that suggested the

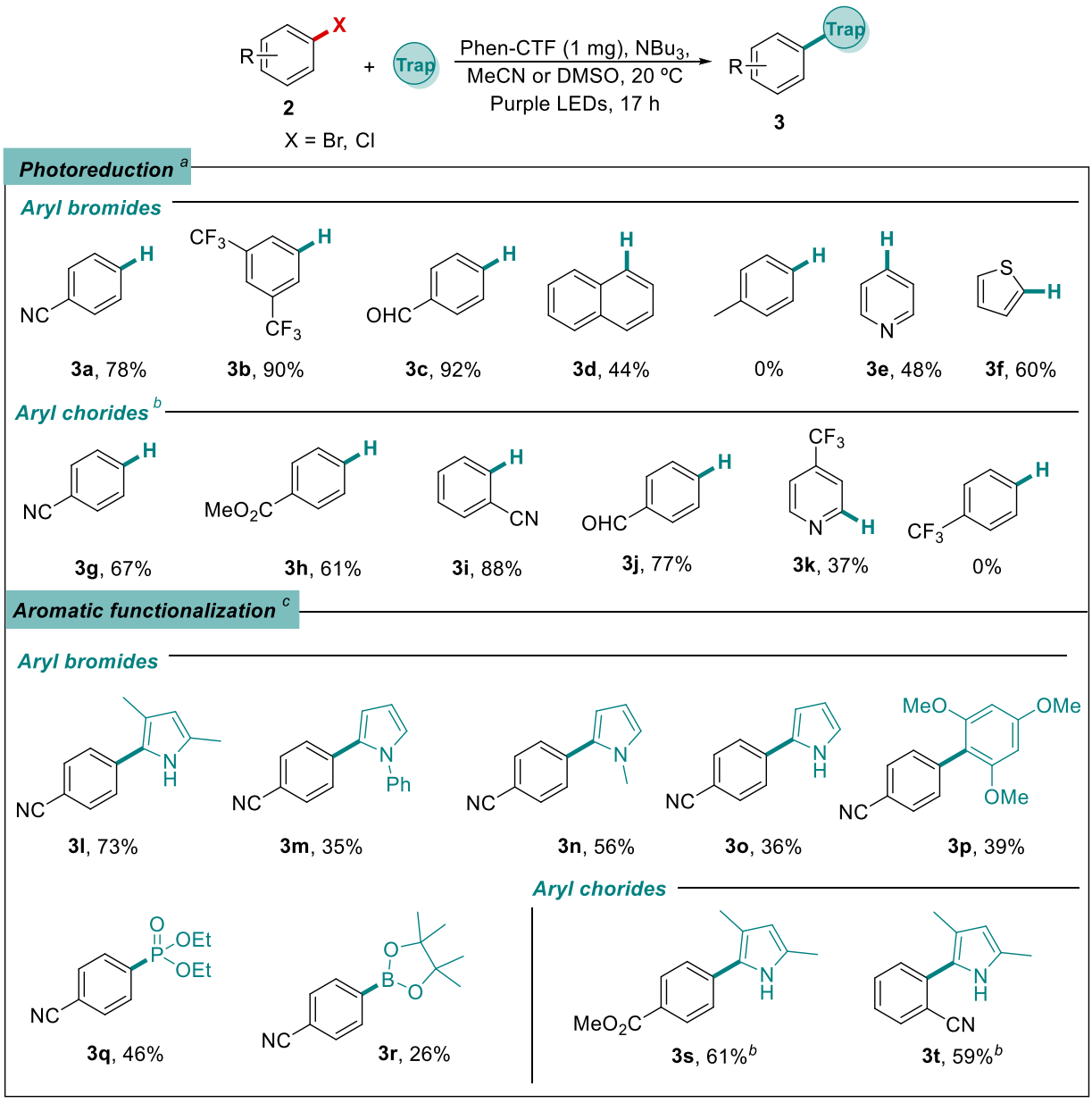

Scheme 1. Light-mediated dehalogenation and trapping reactions catalyzed by **Phen-CTF**. Standard rection conditions: a) Conditions for dehalogenation reactions: 0.1 mmol (Ar-X), NBu_3 (5.0 equiv.), HCOOH (5.0 equiv.), **Phen-CTF** (1.0 mg), MeCN (1.0 mL) under Ar atmosphere and 385 nm LED irradiation. Yields were calculated using 1,3,5-trimethoxybenzene as internal standard. b) Reactions carried out for 72 h. c) Conditions for trapping experiments: 0.1 mmol (Ar-X), NBu_3 (2.0 equiv.), trapping reagent (25.0 equiv.), **Phen-CTF** (1.0 mg), DMSO (1.0 mL) under Ar atmosphere and 385 nm LED irradiation for 17 h. Yields were calculated after chromatographic purification.

existence of diverse excited states raised the question of whether some of this high energy electronic configurations could be used on photoredox processes. A particularly interesting kind of electron transfer reaction induced by light is the C-X (X =Cl, Br) activation [14]. Therefore, we initially decided to employ **Phen-CTF** as heterogeneous photocatalyst in light-mediated dehalogenation reactions. As a model substrate, 4-bromobenzonitrile (**2a**) was employed, using previously reported conditions involving the use of acetonitrile, formic acid and tributylamine (TBA) as sacrificial electron donor [54]. As a result, full conversion was achieved after 17 h of irradiation under purple LEDs (385 nm). In addition we observed in our kinetic studies an induction period ranging from 60 to 90 min (see Fig. S13). This result suggests that this time under this reaction conditions is required to reach a steady-state as a result of the balance between adsorption and diffusion of substrates on the surface of the porous material. Background reactions in absence of catalyst or in dark conditions were discarded through the corresponding control experiments (Table S1 of SI). Moreover, inert atmosphere is indispensable for the correct catalytic outcome, since the presence of oxygen is detrimental for this catalytic system.

Under the optimized conditions in hand, we evaluated the scope of light-mediated dehalogenation reactions by varying the substituents in the aromatic ring (Scheme 1, *photoreduction*). The presence of electron withdrawing substituent decreased the reduction potential of the brominated arenes, thus compounds **3a**, **3b** and **3c** were obtained in very good yields. However, although it was possible to reduce the bromo-naphthalene **2d**, the presence of electron donating substituents such as methyl increased the reduction potential ($E_{red} = -2.2$ V vs. Ag/AgCl, see Fig. S15), and the reaction did not take place. Heteroarene brominated compounds were also examined, being possible to reduce not only the electron deficient pyridine derivative **2e**, but also the

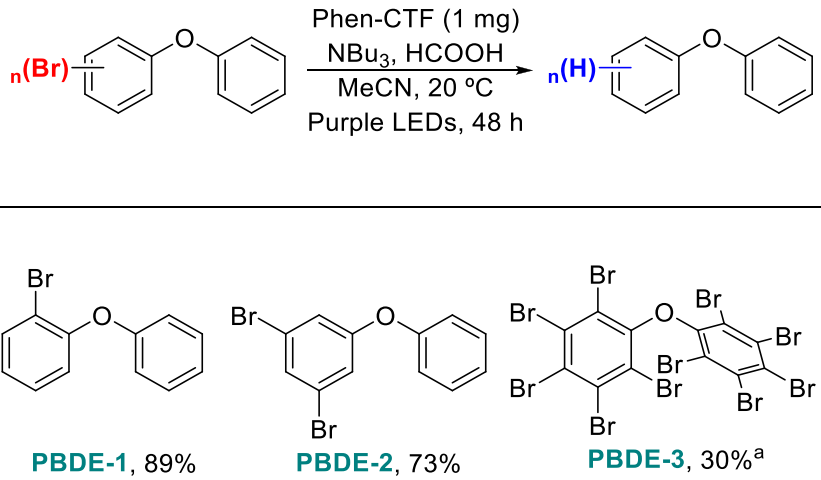

Scheme 2. Light-mediated dehalogenation of Polybromodiphenyl ether (PBDEs). a) This number is referred to the proportion of bromine atoms that were removed from the final product.

thiophene derivative **2f** with a much higher reduction potential (E_{red} = −2.0 V)[6] what also demonstrates the high reduction power of the heterogeneous photocatalyst.

Prompted by these encouraging results in the photocatalytic activation of C-Br bonds, the challenging cleavage of C-Cl bonds was also studied, which are usually harder to activate due to their higher reduction potentials [55]. In fact, only powerful homogeneous photoredox catalysts such as PDI [8], or the biphotonic catalytic system rhodamine 6G [5–7] were able, up to date, to trigger the scission of C-Cl bonds. However, to the best of our knowledge, there are no examples of heterogeneous organic photocatalytic systems able to trigger aryl C-Cl bond cleavage [56] (see Table S4 of Supporting Information). We carried out the reaction with different electron withdrawing substituted aryl chlorides and a good result was obtained with a nitrile in different

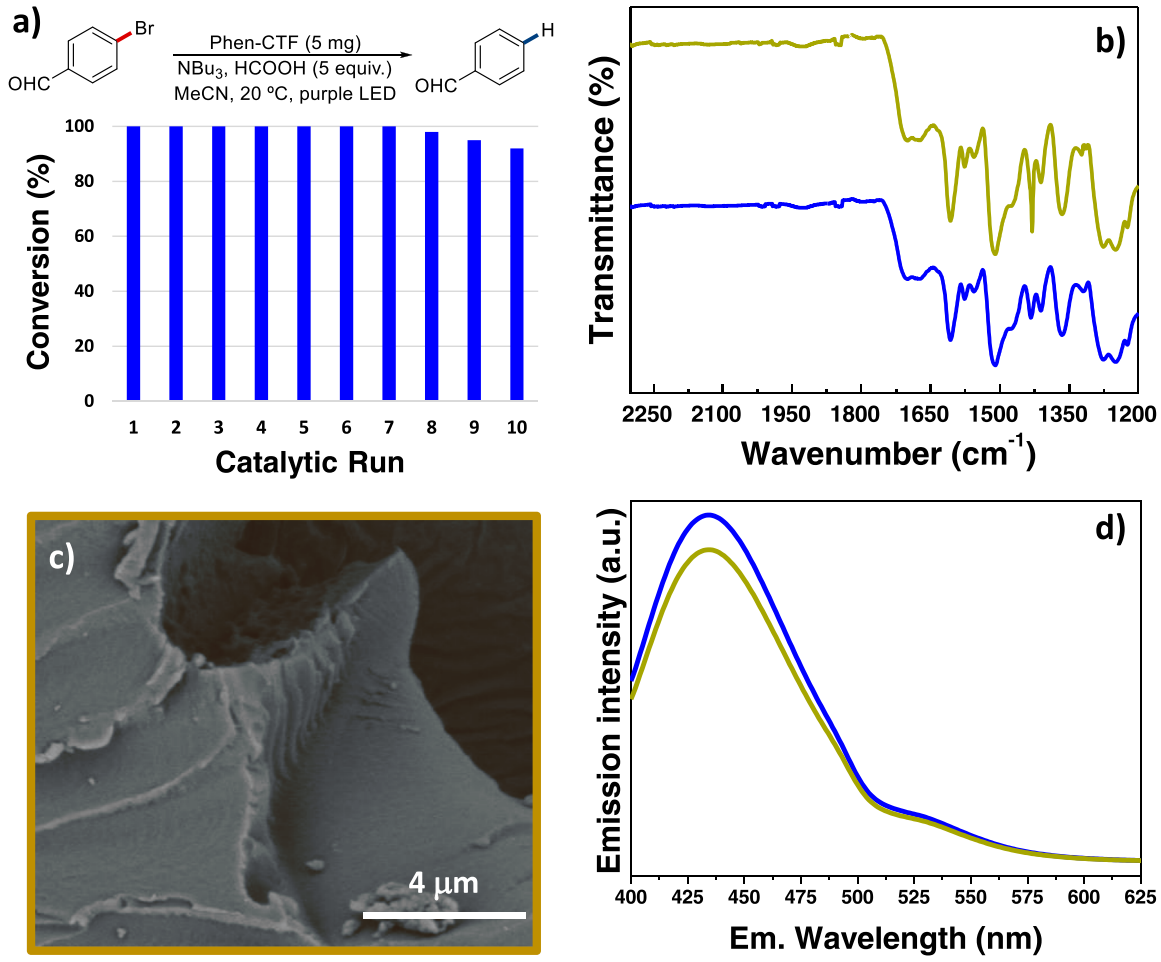

Fig. 4. Recyclability of **Phen-CTF**. a) Catalytic runs. b) Comparison between FTIR spectra of **Phen-CTF** before (blue) and after (brown) catalysis. c) SEM image after catalysis of **Phen-CTF**. d) Comparison between emission spectra of **Phen-CTF** before (blue) and after (brown) catalysis.

Table 1
Dehalogenation reactions performed with other heterogeneous/homogeneous systems similar to **Phen-CTF**.

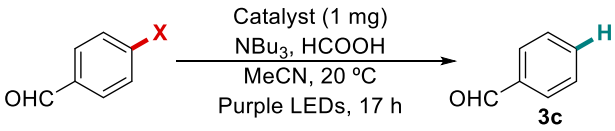

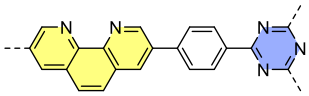

Phen-CTF

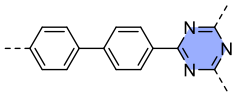

CTF-4

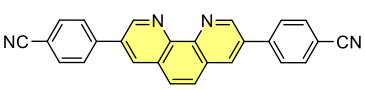

1

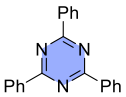

TPT

Entry	Catalyst	X = Br	X = Cl
1	**CTF-4**	34%	n.r.
2	**Phen-CTF**	> 99%	81%
3	TPT	n.r.	n.r.
4	1	n.r.	n.r.
5	TPT + 1	n.r.	n.r.

positions (**3g** and **3i**), an ester (**3h**) or an aldehyde (**3j**) in the structure, even with a pyridine bearing a CF_3 group (**3k**). However, the reduction potential of the aryl chloride with a CF_3 group is too high ($E_{red} = -2.30$ V, see Fig. S15) for the reaction to take place. This result also allowed us to determine the limit of the reduction power of our **Phen-CTF**.

Attending to the good results obtained so far in the photoreduction of halogenated arenes, we envisioned the use of different radical trappings in the reaction for the construction of new C-C, C-P and C-B bonds [57] (Scheme 1, *aromatic functionalization*). We initially studied the formation of new C-C bonds using different (hetero)arenes as trapping reagents [4–6,8,58]. The reaction between the 4-bromobenzonitrile with different pyrrole derivatives (pyrrole, *N*-methylpyrrole, *N*-phenylpyrrole and 2,4-dimethylpyrrole), afforded after 17 h of irradiation compounds **3l**, **3m**, **3n** and **3o** in moderate to good yields. Moreover, the reaction could be carried out with the 1,3,5-trimethoxybenzene as trapping reagent obtaining **3p** in moderate yield [5]. The synthetic applicability of our heterogeneous photocatalytic system could be also widened through the formation of C-B and C-P bonds. Thus, in the presence of triethyl phosphite, **3q** was obtained in moderate yield [59,60]. In addition, in the presence of bis(pinacolato)diboron, **3r** was obtained in a modest 26% yield [61–64]. Furthermore, challenging transient aryl radicals formed through reduction of aryl chlorides could be employed in the formation of C-C bonds, through their reaction with 2,4-dimethylpyrrole, affording **3s** and **3t** in good yields after 72 h of irradiation.

Overall, the catalytic experiments shown above highlight the versatility of **Phen-CTF** in the dehalogenation of aromatic halides and their use in the formation of new C-C, C-B and C-P bonds. Altogether is a remarkable achievement for a unique photocatalytic system.

Beyond the synthetic application of our catalytic system, we applied the versatility of **Phen-CTF** to activate carbon-halogen bonds in the degradation of different polybrominated diphenyl ethers (PBDEs). They are considered as an emergent class of persistent organic pollutants, since they are widely employed as additives to trigger flame retardancy in combustion engines [17]. In such a way, dehalogenation of 1-bromo-2-phenoxybenzene, considered the model substrate of PBDEs because of its high toxicity and simplicity [65], was performed in 89% of yield after 48 h of irradiation. This dehalogenation could also be performed in a mixture of EtOH-H_2O 1:1, reaching a modest 30% of isolated yield after 48 h of irradiation. Moreover, photocatalytic degradation of 1,3-dibromo-5-phenoxybenzene, which bears two bromine groups in the *meta* position, afforded the completely debrominated product in 73% yield. Finally, fully brominated decabromodiphenyl ether was irradiated during 72 h in presence of **Phen-CTF**, affording the loss of 30% of bromine atoms (Scheme 2) (see Supporting Information for further details).

An essential requirement for a heterogeneous catalyst relays on its ability to be reused several times without affecting its structure or chemical identity. Thus, we decided to evaluate the reusability of **Phen-CTF** under typical dehalogenation conditions, using 4-bromobenzaldehyde as substrate. Starting from 5 mg of catalyst, we were able to carry out 10 catalytic cycles with negligible conversion loss (Fig. 4). In terms of product-catalyst ratio, we were able to generate 1 mmol (106 mg) of benzaldehyde with only 5 mg of **Phen-CTF**. The chemical identity, microstructure and photoluminescence of the material were preserved, as it can be inferred from FTIR spectrum, SEM images and emission of the material after catalysis experiments. In addition, we discarded leaching phenomena by filtration of the reaction at 50% of conversion and re-addition of initial substrate, observing no further evolution of the crude in absence of catalyst (Fig. S12 of Supporting Information).

3.2.1. *Comparison and control experiments*

On our way to elucidate why **Phen-CTF** material has optimal photocatalytic activity, we decided to carry out two sets of experiments. First, a comparative catalytic essay employing **Phen-CTF** and **CTF-4** (an analogous material that contains biphenyl structure instead of phenanthroline)[45] was carried out for the light-mediated dehalogenation of 4-bromo and 4-chlorobenzaldehyde (Table 1 and S3 of S.I.). In the case of 4-bromo benzaldehyde, **Phen-CTF** afforded full conversion, while **CTF-4** only reached 34%. In the case of the chlorinated one, **CTF-4** was not capable of triggering the catalytic transformation, while **Phen-CTF** reached 81% (compare entries 1 and 2 of Table 1).

Another experiment consisted of performing homogeneously catalyzed reactions of 4-bromobenzaldehyde in presence of molecular fragments that are present in **Phen-CTF** structure. Thus, the reaction was carried out with 2,4,6-triphenyltriazine (TPT, as a molecular analogue of triazine moieties), building block **1**, and both structures together in the reaction, but no conversion was obtained in any case (Table 1). These results suggest that the catalytic activity observed for **Phen-CTF** arises from the synergistic combination of both triazine and phenanthroline units in the conjugated framework. The incremental catalytic effect of phenanthroline fragment in **Phen-CTF** when compared with **CTF-4** agrees well with previous reports, where similar N-enriched materials had a higher catalytic activity than the carbonaceous analogues for hydrogen production [43,44].

3.2.2. *Mechanistic considerations*

Otherwise, the reduction can take place through two different mechanistic pathways [66]. On the one hand, the excited photocatalyst could directly reduce the aryl halide, and then take an electron form the

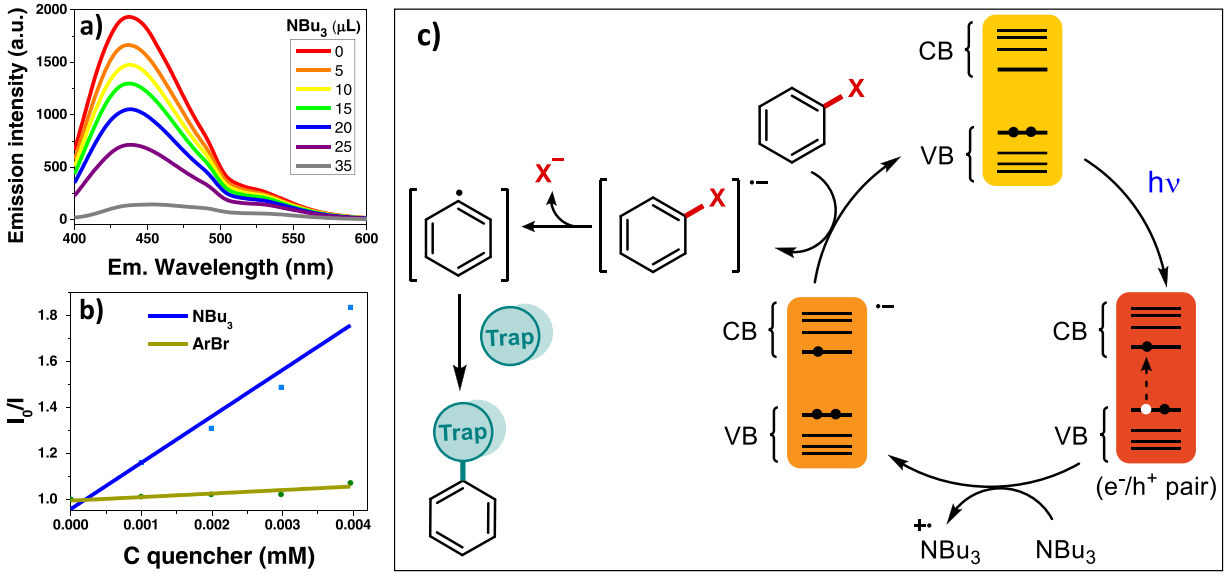

Fig. 5. Mechanistic experiments and proposal. a) Quenching of emission of Phen-CTF by addition of TBA. b) Stern-Volmer plot. c) Proposed mechanism for the light-mediated photoreductive dehalogenations triggered by **Phen-CTF**.

sacrificial electron donor to close the catalytic cycle. On the other hand, the excited state can react with a sacrificial electron donor present in the media forming the corresponding reduced species, that would be responsible for the final reduction of the aryl halide. Fluorescence quenching studies of the excited photocatalyst with the aryl halide and the tributyl amine (TBA) revealed that only the TBA efficiently quenched the excited state of the catalyst (Fig. 5b). Thus, our mechanistic proposal would start with the excitation of Phen-CTF, producing the separation or charges and generating an electron-hole pair system. Then, the sacrificial electron donor is able to give an electron to the valence band of the catalyst, generating the reduced species of Phen-CTF, which is capable of injecting the remaining electron in the conduction band to the aryl halide to form the corresponding radical anion and regenerating the photocatalyst cycle. Upon C-halogen bond scission, the halide is released and the transient aryl radical is formed, that can react with the different radical trapping reagents employed in this work. Additional evidence for aryl radical formation is provided by the experiment using TEMPO as a radical scavenger [67]. Under these conditions, benzonitrile radical-TEMPO adduct has been isolated in 15% yield (see Supporting Information for further details).

4. Conclusions

Cyclotrimerization of 4,4′-(1,10-phenanthroline-3,8-diyl)dibenzonitrile in presence of TFMSA resulted on a novel covalent triazine framework with additional N atoms in its backbone. The conjugated structure (**Phen-CTF**) that combines triazine and phenanthroline units shows enhanced photoluminescence and powerful photoredox properties, which are not observed for its molecular fragments separately. The combined features of this material resulted on an outstanding photocatalytic activity for challenging photoredox processes. In particular, carbon-halogen bond (C-Br and C-Cl) activation under light irradiation triggers dehalogenation processes, and C-C, C-P and C-B bond formation through radical trapping. This photocatalytic material is chemically robust and catalytic reactions can be performed in successive recycling experiments. In addition, this material can be applied to remediation procedures, as shown for degradation of PBDEs. The variety of the catalytic experiments performed in this work highlights the versatility of the material studied. Overall, the results reported herein indicate that highly conjugated CTF materials offer an excellent platform to build photocatalytic frameworks with unprecedented properties that arise from synergistic phenomena. Further developments following this approach could include a variety of synthetic strategies and sewage purification.

CRediT authorship contribution statement

Alberto López-Magano: Investigation, Formal analysis. **Noelia Salaverri:** Investigation, Formal analysis. **Leyre Marzo:** Conceptualization, Writing – review & editing, Supervision. **Rubén Mas-Ballesté**: Conceptualization, Writing – review & editing, Supervision, **Jose Alemán**: Conceptualization, Writing – review & editing, Supervision.

Declaration of Competing Interest

The authors declare that they have no known competing financial interests or personal relationships that could have appeared to influence the work reported in this paper.

Data availability

Data will be made available on request.

Acknowledgments

Financial support was provided by the Spanish Government (RTI2018–095038-B-I00, PID2019–110637RB-I00), “Comunidad de Madrid”, European Structural Funds (S2018/NMT-4367), proyectos sinérgicos I+D (Y2020/NMT6469) and Comunidad Autónoma de Madrid (SI1/PJI/2019–00237). A. L.-M. thanks UAM for a FPI-UAM predoctoral fellowship, N.S. thanks MINECO for a FPU predoctoral fellowship, and L.M. thanks CAM for an “Atracción de Talento Investigador” contract (2017-T2/AMB-5037). We thank María Dolores Navarro-Blanco for the preliminary results.

Appendix A. Supporting information

Supplementary data associated with this article can be found in the online version at doi:10.1016/j.apcatb.2022.121791.

References

[1] N.A. Romero, D.A. Nicewicz, Organic photoredox catalysis, Chem. Rev. 116 (2016) 10075–10166.
[2] J.D. Bell, J.A. Murphy, Recent advances in visible light-activated radical coupling reactions triggered by (i) ruthenium, (ii) iridium and (iii) organic photoredox agents, Chem. Soc. Rev. 50 (2021) 9540–9685.
[3] T.M. Monos, C.R.J. Stephenson, Photoredox Catalysis of Iridium(III)-Based Photosensitizers, Iridium(III) in Optoelectronic and Photonics Applications, 2017: 541–581.
[4] E.H. Discekici, N.J. Treat, S.O. Poelma, K.M. Mattson, Z.M. Hudson, Y. Luo, C. J. Hawker, J.R. de Alaniz, A highly reducing metal-free photoredox catalyst: design and application in radical dehalogenations, Chem. Commun. 51 (2015) 11705–11708.
[5] I. Ghosh, B. König, Chromoselective photocatalysis: controlled bond activation through light-color regulation of redox potentials, Angew. Chem. Int. Ed. 55 (2016) 7676–7679.
[6] L. Marzo, I. Ghosh, F. Esteban, B. König, Metal-free photocatalyzed cross coupling of bromoheteroarenes with pyrroles, ACS Catal. 6 (2016) 6780–6784.
[7] J.M. Haimerl, I. Ghosh, B. König, J.M. Lupton, J. Vogelsang, Chemical Photocatalysis with Rhodamine 6G: Investigation of Photoreduction by Simultaneous Fluorescence Correlation Spectroscopy and Fluorescence Lifetime Measurements, J. Phys. Chem. B 122 (2018) 10728–10735.
[8] I. Ghosh, T. Ghosh, I.B. Javier, B. König, Reduction of aryl halides by consecutive visible light-induced electron transfer processes, Science 346 (2014) 725–728.
[9] I.A. MacKenzie, L. Wang, N.P.R. Onuska, O.F. Williams, K. Begam, A.M. Moran, B. D. Dunietz, D.A. Nicewicz, Discovery and characterization of an acridine radical photoreductant, Nature 580 (2020) 76–80.
[10] A. López-Magano, A. Jiménez-Almarza, J. Alemán, R. Mas-Ballesté, Metal–Organic Frameworks (MOFs) and Covalent Organic Frameworks (COFs) Applied to Photocatalytic Organic Transformations, Catalysts 10 (2020) 720.
[11] A. López-Magano, B. Ortín-Rubio, I. Imaz, D. Maspoch, J. Alemán, R. Mas-Ballesté, Photoredox heterobimetallic dual catalysis using engineered covalent organic frameworks, ACS Catal. 11 (2021) 12344–12354.
[12] B. Qiao, Z. Jiang, Catalytic photoreduction induced by visible light, ChemPhotoChem 2 (2018) 703–714.
[13] M. Cybularczyk-Cecotka, J. Szczepanik, M. Giedyk, Photocatalytic strategies for the activation of organic chlorides, Nat. Catal. 3 (2020) 872–886.
[14] N. Kvasovs, V. Gevorgyan, Contemporary methods for generation of aryl radicals, Chem. Soc. Rev. 50 (2021) 2244–2259.
[15] I. Ghosh, L. Marzo, A. Das, R. Shaikh, B. König, Visible light mediated photoredox catalytic arylation reactions, Acc. Chem. Res. 49 (2016) 1566–1577.
[16] H. Kim, C. Lee, Visible-light-induced photocatalytic reductive transformations of organohalides, Angew. Chem. Int. Ed. 51 (2012) 12303–12306.
[17] B. Yao, Z. Luo, D. Zhi, D. Hou, L. Luo, S. Du, Y. Zhou, Current progress in degradation and removal methods of polybrominated diphenyl ethers from water and soil: A review, J. Hazard. Mater. 403 (2021), 123674.
[18] Z. Qian, K.A.I. Zhang, Recent advances of conjugated microporous polymers in visible light–promoted chemical transformations, Sol. RRL 5 (2021), 2000489.
[19] X. Kang, X. Wu, X. Han, C. Yuan, Y. Liu, Y. Cui, Rational synthesis of interpenetrated 3D covalent organic frameworks for asymmetric photocatalysis, Chem. Sci. 11 (2020) 1494–1502.
[20] Z. Li, Y. Zhi, P. Shao, H. Xia, G. Li, X. Feng, X. Chen, Z. Shi, X. Liu, Covalent organic framework as an efficient, metal-free, heterogeneous photocatalyst for organic transformations under visible light, Appl. Catal. B: Environ. 245 (2019) 334–342.
[21] H. Shan, D. Cai, X. Zhang, Q. Zhu, P. Qin, J. Baeyens, Donor-acceptor type two-dimensional porphyrin-based covalent organic framework for visible-light-driven heterogeneous photocatalysis, Chem. Eng. J. 432 (2022), 134288-134288.
[22] A. Jiménez-Almarza, A. López-Magano, R. Cano, B. Ortín-Rubio, D. Díaz-García, S. Gomez-Ruiz, I. Imaz, D. Maspoch, R. Mas-Ballesté, J. Alemán, Engineering covalent organic frameworks in the modulation of photocatalytic degradation of pollutants under visible light conditions, Mater. Today Chem. 22 (2021), 100548.
[23] W. Zhang, J. Deng, Z. Fang, D. Lan, Y. Liao, X. Zhou, Q. Liu, Promoting charge separation in donor–acceptor conjugated microporous polymers via cyanation for the photocatalytic reductive dehalogenation of chlorides, Catal. Sci. Technol. 11 (2021) 7151–7159.
[24] J. Luo, X. Zhang, J. Zhang, Carbazolic porous organic framework as an efficient, metal-free visible-light photocatalyst for organic synthesis, ACS Catal. 5 (2015) 2250–2254.
[25] W. Huang, B.C. Ma, D. Wang, Z.J. Wang, R. Li, L. Wang, K. Landfester, K.A. I. Zhang, A fixed-bed photoreactor using conjugated nanoporous polymer-coated glass fibers for visible light-promoted continuous photoredox reactions, J. Mater. Chem. A 5 (2017) 3792–3797.
[26] M. Liu, L. Guo, S. Jin, B. Tan, Covalent triazine frameworks: synthesis and applications, J. Mater. Chem. A 7 (2019) 5153–5172.
[27] Y. Zhang, S. Jin, Recent advancements in the synthesis of covalent triazine frameworks for energy and environmental applications, Polymers 11 (2019) 31.
[28] F. Li, D. Wang, Q.-J. Xing, G. Zhou, S.-S. Liu, Y. Li, L.-L. Zheng, P. Ye, J.-P. Zou, Design and syntheses of MOF/COF hybrid materials via postsynthetic covalent modification: An efficient strategy to boost the visible-light-driven photocatalytic performance, Appl. Catal. B: Environ. 243 (2019) 621–628.
[29] D. Wang, H. Zeng, X. Xiong, M.-F. Wu, M. Xia, M. Xie, J.-P. Zou, S.-L. Luo, Highly efficient charge transfer in CdS-covalent organic framework nanocomposites for stable photocatalytic hydrogen evolution under visible light, Sci. Bull. 65 (2020) 113–122.
[30] C. Wu, X. Li, M. Shao, J. Kan, G. Wang, Y. Geng, Y.-B. Dong, Porphyrin covalent organic framework for photocatalytic synthesis of tetrahydroquinolines, Chin. Chem. Lett. 33 (2022) 4559–4562.
[31] H. Hao, F. Zhang, X. Dong, X. Lang, 2D sp2 carbon-conjugated triazine covalent organic framework photocatalysis for blue light-induced selective oxidation of sulfides with O2, Appl. Catal. B: Environ. 299 (2021), 120691-120691.
[32] X. Wang, S. Zhang, X. Li, Z. Zhan, B. Tan, X. Lang, S. Jin, Two-dimensional crystalline covalent triazine frameworks via dual modulator control for efficient photocatalytic oxidation of sulfides, J. Mater. Chem. A 9 (2021) 16405–16410.
[33] B. Wu, Y. Liu, Y. Zhang, L. Fan, Q.-Y. Li, Z. Yu, X. Zhao, Y.-C. Zheng, X.-J. Wang, Molecular engineering of covalent triazine frameworks for highly enhanced photocatalytic aerobic oxidation of sulfides, J. Mater. Chem. A 10 (2022) 12489–12496.
[34] T. Xu, Y. Li, Z. Zhao, G. Xing, L. Chen, N,N′,Bicarbazole-Based Covalent Triazine Frameworks as High-Performance Heterogeneous Photocatalysts, Macromolecules 52 (2019) 9786–9791.
[35] B. Fuerte-Díez, A. Valverde-González, M. Pintado-Sierra, U. Díaz, F. Sánchez, E. M. Maya, M. Iglesias, Phenyl Extended Naphthalene-Based Covalent Triazine Frameworks as Versatile Metal-Free Heterogeneous Photocatalysts, Sol. RRL 6 (2022), 2100848.
[36] W. Huang, B.C. Ma, H. Lu, R. Li, L. Wang, K. Landfester, K.A.I. Zhang, Visible-Light-Promoted Selective Oxidation of Alcohols Using a Covalent Triazine Framework, ACS Catal. 7 (2017) 5438–5442.
[37] L. Liao, D. Ditz, F. Zeng, M. Alves Favaro, A. Iemhoff, K. Gupta, H. Hartmann, C. Szczuka, P. Jakes, P.J.C. Hausoul, J. Artz, R. Palkovits, Efficient photocatalytic oxidation of aromatic alcohols over thiophene-based covalent triazine frameworks with a narrow band gap, ChemistrySelect 5 (2020) 14438–14446.
[38] X. Lan, X. Liu, Y. Zhang, Q. Li, J. Wang, Q. Zhang, G. Bai, Unveiling Charge Dynamics in Acetylene-Bridged Donor−π–Acceptor Covalent Triazine Framework for Enhanced Photoredox Catalysis, ACS Catal. 11 (2021) 7429–7441.
[39] A. Jiménez-Almarza, A. López-Magano, R. Mas-Ballesté, J. Alemán, Tuning the Activity–Stability Balance of Photocatalytic Organic Materials for Oxidative Coupling Reactions, ACS Appl. Mater. Interfaces 14 (2022) 16258–16268.
[40] Y. Zou, S. Abednatanzi, P. Gohari Derakhshandeh, S. Mazzanti, C.M. Schüßlbauer, D. Cruz, P. Van Der Voort, J.-W. Shi, M. Antonietti, D.M. Guldi, A. Savateev, Red edge effect and chromoselective photocatalysis with amorphous covalent triazine-based frameworks, Nat. Commun. 13 (2022) 2171.
[41] W. Huang, J. Byun, I. Rörich, C. Ramanan, P.W.M. Blom, H. Lu, D. Wang, L. Caire da Silva, R. Li, L. Wang, K. Landfester, K.A.I. Zhang, Asymmetric covalent triazine framework for enhanced visible-light photoredox catalysis via energy transfer cascade, Angew. Chem. Int. Ed. 57 (2018) 8316–8320.
[42] W. Huang, N. Huber, S. Jiang, K. Landfester, K.A.I. Zhang, Covalent triazine framework nanoparticles via size-controllable confinement synthesis for enhanced visible-light photoredox catalysis, Angew. Chem. Int. Ed. 59 (2020) 18368–18373.
[43] M. Alves Fávaro, D. Ditz, J. Yang, S. Bergwinkl, A.C. Ghosh, M. Stammler, C. Lorentz, J. Roeser, E.A. Quadrelli, A. Thomas, R. Palkovits, J. Canivet, F. M. Wisser, Finding the Sweet Spot of Photocatalysis—A Case Study Using Bipyridine-Based CTFs, ACS Appl. Mater. Interfaces 14 (2022) 14182–14192.
[44] F. Liu, Z. Ma, Y. Deng, M. Wang, P. Zhou, W. Liu, S. Guo, M. Tong, D. Ma, Tunable Covalent Organic Frameworks with Different Heterocyclic Nitrogen Locations for Efficient Cr(VI) Reduction, Escherichia coli Disinfection, and Paracetamol Degradation under Visible-Light Irradiation, Environ. Sci. Technol. 55 (2021) 5371–5381.
[45] C.B. Meier, R.S. Sprick, A. Monti, P. Guiglion, J.-S.M. Lee, M.A. Zwijnenburg, A. I. Cooper, Structure-property relationships for covalent triazine-based frameworks: The effect of spacer length on photocatalytic hydrogen evolution from water, Polymer 126 (2017) 283–290.
[46] A. López-Magano, R. Mas-Ballesté, J. Alemán, Predesigned Covalent Organic Frameworks as Effective Platforms for Pd(II) Coordination Enabling Cross-Coupling Reactions under Sustainable Conditions, Adv. Sustain. Syst. 6 (2022), 2100409.
[47] G. Accorsi, A. Listorti, K. Yoosaf, N. Armaroli, 1,10-Phenanthrolines: versatile building blocks for luminescent molecules, materials and metal complexes, Chem. Soc. Rev. 38 (2009) 1690–1700.
[48] P. Kuhn, M. Antonietti, A. Thomas, Porous, covalent triazine-based frameworks prepared by ionothermal synthesis, Angew. Chem. Int. Ed. 47 (2008) 3450–3453.
[49] R. Luo, W. Xu, M. Chen, X. Liu, Y. Fang, H. Ji, Covalent Triazine Frameworks Obtained from Nitrile Monomers for Sustainable CO_2 Catalysis, ChemSusChem 13 (2020) 6509–6522.
[50] X. Zhu, C. Tian, S.M. Mahurin, S.-H. Chai, C. Wang, S. Brown, G.M. Veith, H. Luo, H. Liu, S. Dai, A Superacid-Catalyzed Synthesis of Porous Membranes Based on Triazine Frameworks for CO_2 Separation, J. Am. Chem. Soc. 134 (2012) 10478–10484.
[51] X. Hu, Z. Zhan, J. Zhang, I. Hussain, B. Tan, Immobilized covalent triazine frameworks films as effective photocatalysts for hydrogen evolution reaction, Nat. Commun. 12 (2021) 6596.
[52] A. Shafiee, M.M. Salleh, M. Yahaya, Determination of HOMO and LUMO of [6,6]-phenyl C61-butyric acid 3-ethylthiophene ester and poly (3-octyl-thiophene-2, 5-diyl) through voltametry characterization, Sains Malays. 40 (2011) 173–176.
[53] J. Pommerehne, H. Vestweber, W. Guss, R.F. Mahrt, H. Bässler, M. Porsch, J. Daub, Efficient two layer leds on a polymer blend basis, Adv. Mater. 7 (1995) 551–554.
[54] D. González-Muñoz, A. Martín-Somer, K. Strobl, S. Cabrera, P.J. De Pablo, S. Díaz-Tendero, M. Blanco, J. Alemán, Enhancing Visible-Light Photocatalysis via Endohedral Functionalization of Single-Walled Carbon Nanotubes with Organic Dyes, ACS Appl. Mater. Interfaces 13 (2021) 24877–24886.

[55] N.G.W. Cowper, C.P. Chernowsky, O.P. Williams, Z.K. Wickens, Potent Reductants via Electron-Primed Photoredox Catalysis: Unlocking Aryl Chlorides for Radical Coupling, J. Am. Chem. Soc. 142 (2020) 2093–2099.
[56] L.-L. Liao, L. Song, S.-S. Yan, J.-H. Ye, D.-G. Yu, Highly reductive photocatalytic systems in organic synthesis, Trends Chem. 4 (2022) 512–527.
[57] M. Neumeier, D. Sampedro, M. Májek, V.A. de la Peña O'Shea, A. Jacobi von Wangelin, R. Pérez-Ruiz, Dichromatic Photocatalytic Substitutions of Aryl Halides with a Small Organic Dye, Chem. – A Eur. J. 24 (2018) 105–108.
[58] Z.-J. Li, S. Li, E. Hofman, A. Hunter Davis, G. Leem, W. Zheng, Visible-light induced disproportionation of pyrrole derivatives for photocatalyst-free aryl halides reduction, Green. Chem. 22 (2020) 1911–1918.
[59] R.S. Shaikh, S.J.S. Düsel, B. König, Visible-light photo-arbuzov reaction of aryl bromides and trialkyl phosphites yielding aryl phosphonates, ACS Catal. 6 (2016) 8410–8414.
[60] H. Zeng, Q. Dou, C.-J. Li, Photoinduced Transition-Metal-Free Cross-Coupling of Aryl Halides with H-Phosphonates, Org. Lett. 21 (2019) 1301–1305.
[61] N. Shen, R. Li, C. Liu, X. Shen, W. Guan, R. Shang, Photocatalytic Cross-Couplings of Aryl Halides Enabled by o-Phosphinophenolate and o-Phosphinothiophenolate, ACS Catal. 12 (2022) 2788–2795.
[62] K. Chen, S. Zhang, P. He, P. Li, Efficient metal-free photochemical borylation of aryl halides under batch and continuous-flow conditions, Chem. Sci. 7 (2016) 3676–3680.
[63] A. Nitelet, D. Thevenet, B. Schiavi, C. Hardouin, J. Fournier, R. Tamion, X. Pannecoucke, P. Jubault, T. Poisson, Copper-Photocatalyzed Borylation of Organic Halides under Batch and Continuous-Flow Conditions, Chem. – A Eur. J. 25 (2019) 3262–3266.
[64] D.S. Lee, C.S. Kim, N. Iqbal, G.S. Park, K.-s Son, E.J. Cho, Organophotocatalytic Arene Functionalization: C–C and C–B Bond Formation, Org. Lett. 21 (2019) 9950–9953.
[65] U. Gill, I. Chu, J.J. Ryan, M. Feeley, Polybrominated diphenyl ethers: human tissue levels and toxicology, Rev. Environ. Contam. Toxicol. 183 (2004) 55–97.
[66] A. Casado-Sánchez, M. Uygur, D. González-Muñoz, F. Aguilar-Galindo, J.L. Nova-Fernández, J. Arranz-Plaza, S. Díaz-Tendero, S. Cabrera, O.G. Mancheño, J. Alemán, 8-Mercaptoquinoline as a Ligand for Enhancing the Photocatalytic Activity of Pt(II) Coordination Complexes: Reactions and Mechanistic Insights, J. Org. Chem. 84 (2019) 6437–6447.
[67] S. Yang, M. Chen, P. Tang, Visible-light photoredox-catalyzed and copper-promoted trifluoromethoxylation of arenediazonium tetrafluoroborates, Angew. Chem. Int. Ed. 58 (2019) 7840–7844.